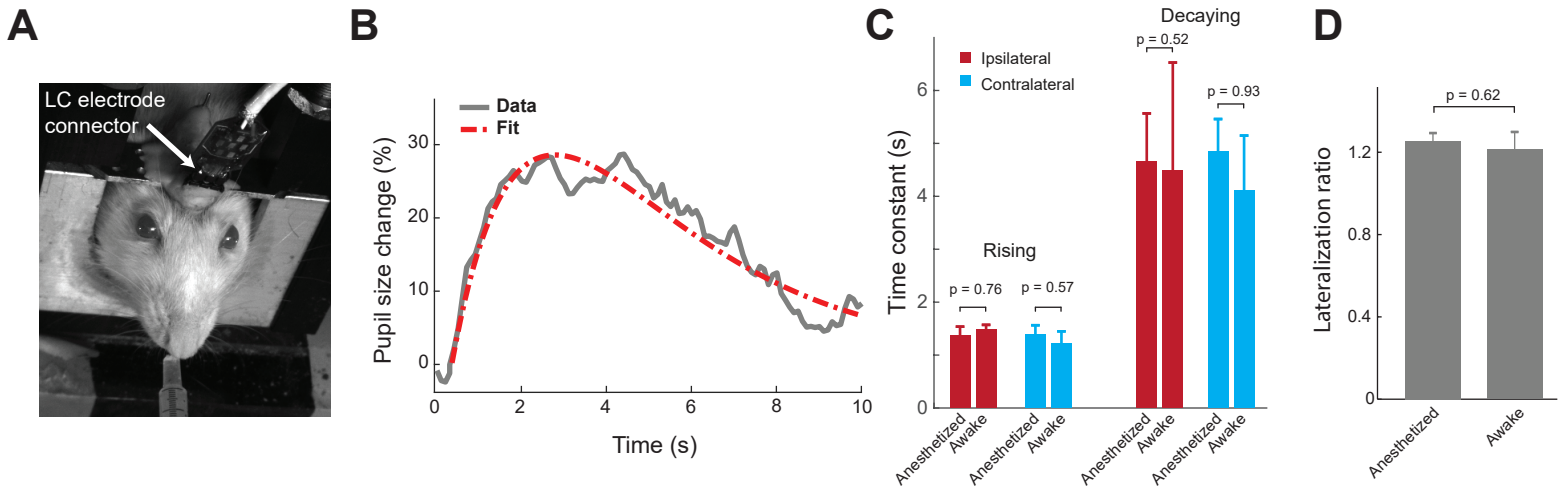

Figure S1. Pupil dilation in response to 50 Hz phasic LC stimulation in awake animals is similar to that in lightly anesthetized animals, Related to Figure 1. A) Photo of an awake, head-constrainted rat with an electrode implanted in the LC. **B)** Example of pupil dilation in response to 50 Hz phasic LC stimulation in an awake animal. **C)** The time course of pupil dilation evoked by 50 Hz phasic LC stimulation was not significantly different between anesthetized and awake animals. **D)** 50 Hz phasic LC stimulation induced similar lateralization in pupil dilation for anesthetized and awake animals.

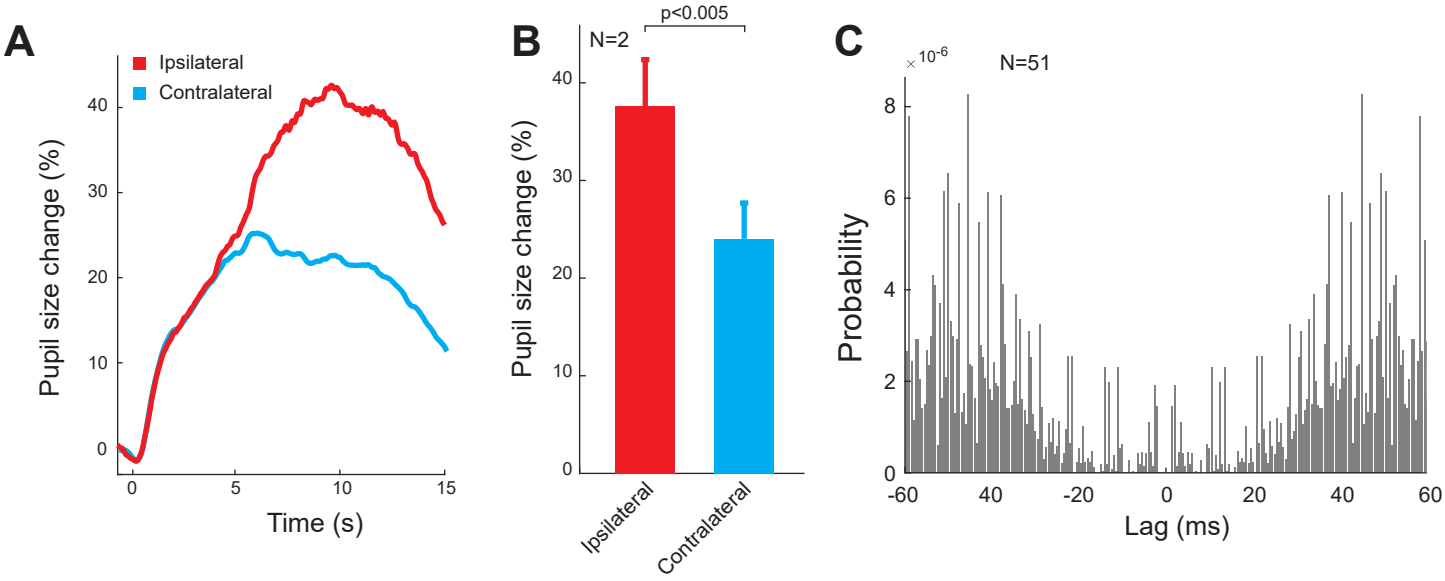

Figure S2. Pupil dilation and LC activity in response to paw pinch, Related to Figure 2. A) Example bilateral pupil dilation evoked by a paw pinch. **B)** Average pupil dilation evoked by a paw pinch for the bilateral pupils. **C)** Autocorrelogram of single-unit LC activity in response to paw pinches exhibited zero probability around lag 0. Bin width: 0.5 ms. Error bars: SEM.

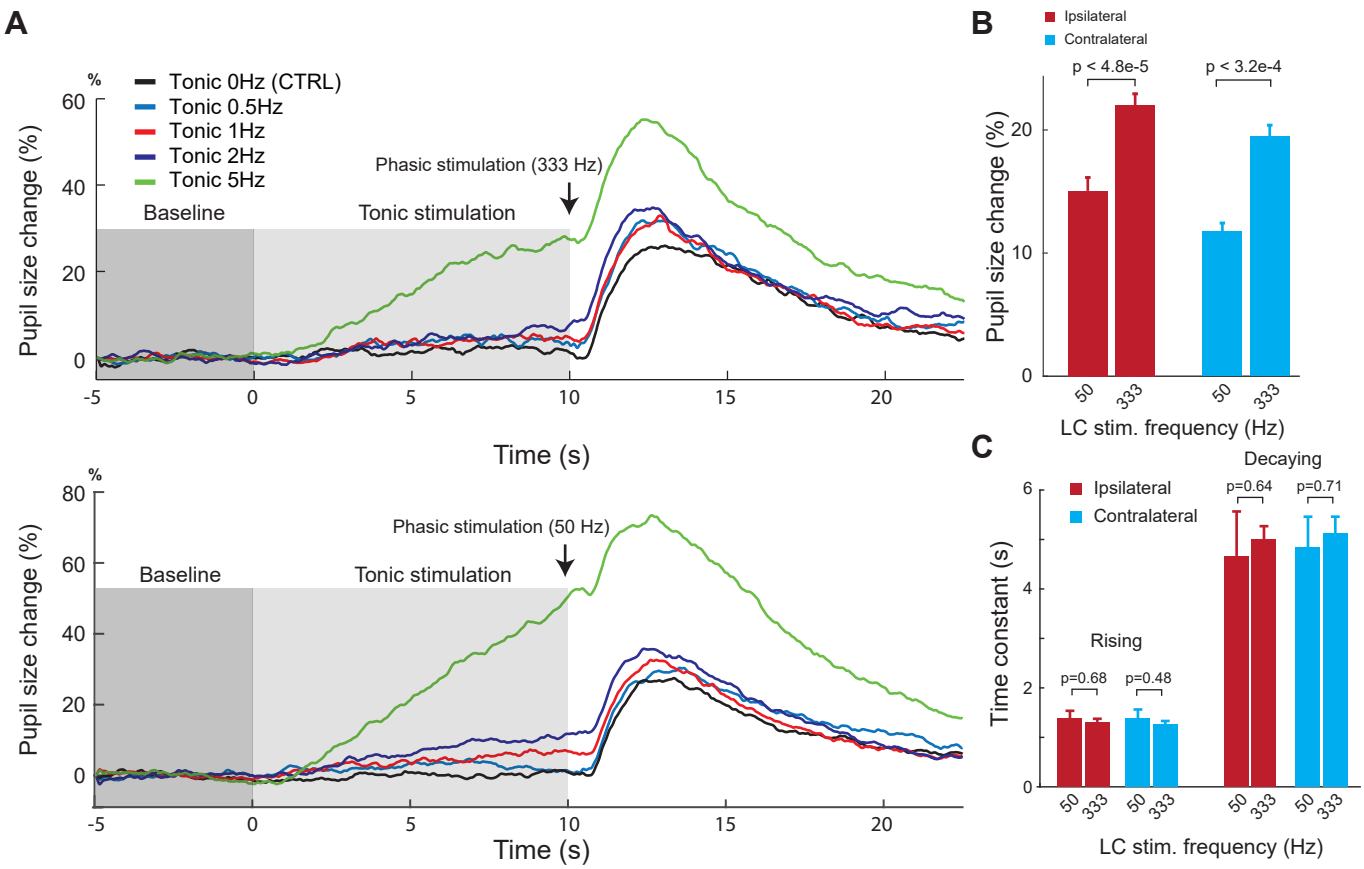

Figure S3. Pupil dilation in response to 50 Hz and 333 Hz phasic LC stimulation, Related to Figure 4. **A)** Example changes in pupil size showing pupil dilation evoked by phasic LC stimulation with an interstimulus-interval of 3ms (top) and 20 ms (bottom). **B)** Pupil dilations in response to 50 Hz LC stimulation is smaller than those to 333 Hz LC stimulation for bilateral pupils. **C)** Time constants of pupil dilation in response to 50 Hz LC stimulation are not significantly different than those to 333 Hz LC stimulation for bilateral pupils.

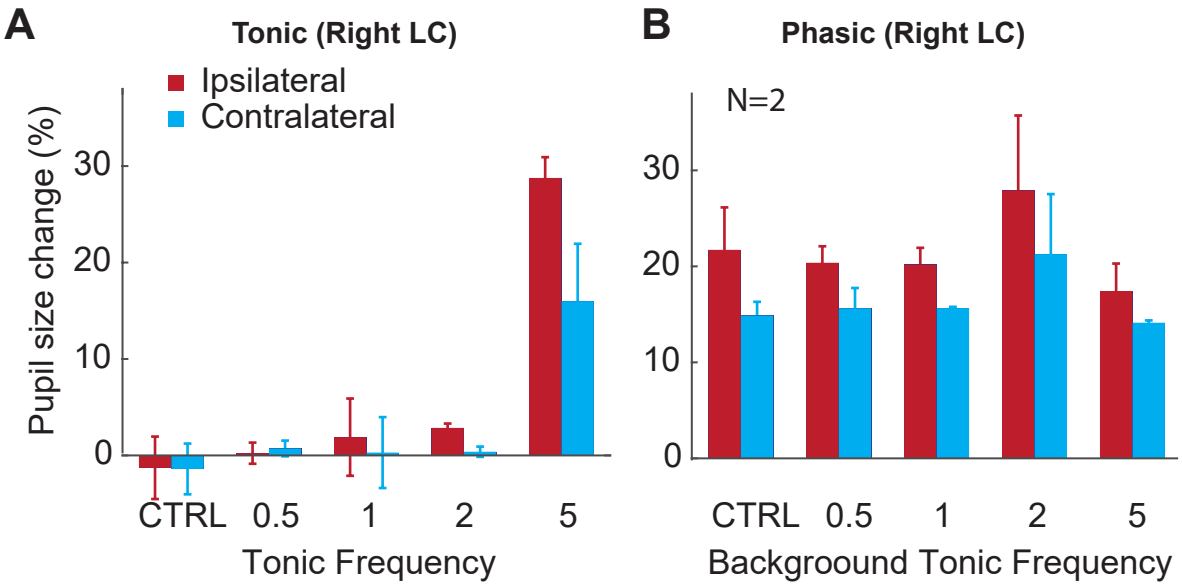

Figure S4. The ipsilateral and contralateral pupils' responses to tonic (A) and phasic stimulation (B) of the right LC are qualitatively similar to that of the left LC, Related to Figure 4.

Supplemental Experimental Procedures

Surgery and preparation. All procedures performed on animals were approved by the Institutional Animal Care and Use Committees at Columbia University, and were conducted in compliance with guidelines of the National Institutes of Health. 56 adult Sprague-Dawley rats weighing between 225 and 300 g (Charles River Laboratories, Wilmington, MA) were used in this study. 50 of the animals were used in acute experiments, while the remaining 6 animals were trained to tolerate head fixation (3 of which were implanted with a platinum/iridium electrode in the LC), allowing for the collection of pupillary light reflex measurements and LC-activation-evoked-pupil-dilation in awake animals.

For acute experiments, all surgeries and LC stimulation were carried out under light isoflurane anesthesia. Surgical procedures were similar to those previously described in detail (Wang et al., 2012; Zheng et al., 2015). Briefly, the animal was initially sedated with 2% vaporized isoflurane in its home cage, before being transported to the experimental suite. The level of isoflurane was maintained at 1.5-2% during craniotomy and ~1% during subsequent LC electrophysiological recording and electrical microstimulation/pupillometry recording. Body temperature was maintained at 37 °C by a servo-controlled heating pad (FHC Inc, Bowdoin, ME). Blood oxygen saturation level and heart rate were continuously monitored using a non-invasive monitor (Nonin Medical Inc, MN). Artificial eye drops (Refresh Liquigel, Allergan, CA) were used to protect the corneas from dehydration.

The animal was mounted on a custom-modified stereotaxic frame (RWD Life Science, China) on top of a floating air table in preparation for the surgery and subsequent LC microstimulation and pupillometry recordings. To allow for placement of a microelectrode within the LC, the head was tilted 15 degrees downward (Devilbiss and Waterhouse, 2004; Vazey and Aston-Jones, 2014) and a small craniotomy was made on the left (n=40) or right (n=2) hemisphere over the LC (stereotaxic coordinates: 3.1-3.7 mm caudal to the Lambda, 1.2-1.4 mm lateral to the midline, and 5.2-6.2 mm deep from the brain surface). After craniotomy, the brain surface was covered with warm saline contained by a retaining well. At the end of the experiment, the animal was deeply anesthetized with an overdose of sodium pentobarbital and a DC current (200 µA, 10 s) was passed through the stimulating electrode every 500 µm during retraction to create lesions, visible in histology. The animal was subsequently transcardially perfused with 4% paraformaldehyde, and the brain was harvested for post-experiment histological analysis.

For chronic implantations, a sterile platinum/iridium microelectrode (~1 MΩ FHC Inc, Bowdoin, ME) was first advanced to the LC. Once the microelectrode's placement in the LC was confirmed based on electrophysiology (see below), the electrode was bonded to a head-plate using dental cement and connected to a connector cemented in the headcap (Figure S1).

Electrophysiological recording. Single-unit extracellular recordings were obtained by using single, sharp tungsten microelectrodes (75 µm in diameter, 1-2 MΩ, FHC Inc, Bowdoin, ME). During electrophysiological recording, the microelectrode was slowly advanced into the LC using a hydraulic micropositioner (David Kopf, CA) (Wang et al., 2010). LC activity was determined based on criteria used in previous studies (Akaike, 1982; Vazey and Aston-Jones, 2014) as follows: 1) wide action potential waveform (>1.8 ms), 2) low spontaneous firing rate (1-5 Hz), 3) elevated firing rate in response to paw or tail pinch, and 4) depth from the brain surface (5.2 – 6.2 mm). Microelectrode placement in the LC was further confirmed by histological analysis, which showed DC current-induced lesions in the LC for all datasets included in this study. Extracellular neural signals were band-pass filtered (300-8k Hz) and sampled at 40 kHz using a Plexon recording system (OmniPlex, Plexon Inc., Dallas, TX).

EEG signals were recorded from a contralateral frontal cortex screw referenced to a screw over the contralateral occipital cortex. EEG signals were filtered (0.1–300 Hz) through a differential amplifier (Model 3000, A-M systems, Sequim, WA), and digitized at 5 kHz using the Plexon system.

Pupillometry recording. Simultaneous recordings of both pupils were made using two pupillometry systems assembled in-house (DMK 23U618, Imaging Source, Germany or FL3-U3-13Y3M-C, Point Grey, BC, Canada), which were triggered by an xPC target real-time system (Mathworks, MA), and were streamed to high-speed solid-state drives. For LC stimulation experiments, eyelids of the animal were gently held open by eyelid retractors, and images of both pupils were collected at 50 Hz. Light intensity was adjusted so that the illuminance at both eyes was measured to be 50 lux (PM 100, Thorlabs, NJ).

Prior to surgery, the pupillary light reflex was measured in 4 isoflurane anesthetized animals. Ambient illuminance was switched between 15 lux and 150 lux every 20 s. The animal's left pupil's dilation and constriction responses to the changes in illuminance were imaged at 50 Hz.

To allow for quantification of the pupillary light reflex in awake animals, three rats were first trained to tolerate head-fixation for >30 min (Ollerenshaw et al., 2012; Bari et al., 2013; Ollerenshaw et al., 2014). Once this was achieved, the pupillary light reflex of the left eye was measured for each rat, while ambient illuminance was switched between 15 lux and 150 lux every 20 s. Pupil dilation and constriction in response to changes in illuminance were imaged at 30 Hz.

LC microstimulation. In acute setups, after confirming the microelectrode's placement in the LC, the microelectrode was disconnected from the recording system and connected to a calibrated electrical microstimulator (Multi Channel Systems, Germany or PSIU6 and S88, Grass Instrument, RI). The microstimulator was triggered by the same real-time system which controlled the pupillometry systems. 50 Hz cathode-leading biphasic current pulses (6 pulses, 200 µs per phase, 60 µA or 120 µA) were found to evoke quantifiable changes in EEG pattern. Since jaw twitching is an indicator of current spreading to the neighboring mesencephalic trigeminal (Me5) nucleus (Aston-Jones et al., 1991), during LC stimulation, close attention was paid to the jaw to confirm that no visible jaw twitching occurred in response to the LC stimulation.

For each EEG experiment the stimulation was delivered 12 times, with a one-minute rest interval between activations, and with EEG recordings acquired before and after stimulation. For evoking pupil dilation, cathode-leading biphasic current pulses (200 µs per phase, 60 µA amplitude) were delivered to the LC as a basic stimulus unit. Each stimulus block consisted of 5 s of baseline (i.e. no LC stimulation) followed by 10 s of tonic LC stimulation with different frequencies (0, 0.5, 1, 2, and 5 Hz), this was then followed by a phasic LC stimulation (50 Hz or 330 Hz, 6 pulses). These stimulus blocks (Figure 3A) were delivered in an interleaved fashion with 60 s between each block. Approximately 36 trials were collected for each experiment.

In awake setups, once the animal was trained to tolerate head-fixation for >45 minutes (~4-6 weeks following implantation), 50 Hz cathode-leading biphasic current pulses (6 pulses, 200 µs per phase) were delivered to the implanted LC electrode every 60-120 seconds, with a random delivery of a drop of Kool-aid solution occurring 20-40 seconds before stimulation. Since we found that current with an amplitude < 100 µA evoked no distinguishable pupil dilation from background noise, presumably due to scar tissue formation around the electrode, we used 150 µA for all three animals.

Superior cervical ganglionectomy (SCGx). The SCG was removed on either the right (n=12) or the left (n=13) side before craniotomy using a procedure described in detail previously (Savastano et al., 2010). Briefly, the animal was laid on its back on top of the heating pad. After shaving the neck region, a 3.0 cm vertical incision along the midline was made to expose the mandibular glands. Connective tissue was separated in the middle of the mandibular glands to expose the sternohyoid muscle. The sternohyoid and omohyoid muscles were carefully separated to expose the lymph node and carotid artery. At the bifurcation of the carotid artery, the external and internal carotid artery were carefully separated from the SCG underneath. Extreme care was taken to not damage the vagus nerve. The pre and post-ganglion branches of the SCG were cut to allow for its removal, followed by its fixation in 4% paraformaldehyde for immunohistochemistry.

Pharmacological inactivation of EWN. In 4 animals, the adrenergic antagonist yohimbine was injected into the ipsilateral EWN to inhibit the influence of LC on the parasympathetic pathway. In the yohimbine solution, 2% w/v Lucifer Yellow (Thermo Fisher Scientific, Waltham, MA) was added to visualize the extent of yohimbine solution diffusion in the brain tissue. Following craniotomy and removal of dura matter, 1 µL of 0.5 mM or 1 mM Yohimbine was injected using a pulled glass pipette (~30 µm tip diameter) and a PLI-100 pressure injector (Harvard Apparatus, Holliston, MA) into the EWN according to the positions on Rat Brain Atlas (Paxinos and Watson, 2009) at 0.2 mm lateral, 6.3 mm posterior, and 6.0 mm deep relative to Bregma. To avoid the superior sagittal sinus, the glass pipette was tilted 10 degrees.

Immunohistochemistry. Nissl staining was used to verify placement of the electrode tip in the LC. The animal's brain was removed following perfusion with 4% paraformaldehyde, fixed in 4% paraformaldehyde in phosphate buffered saline (PBS) for up to 24 hours at 4˚C, and cryoprotected in increasing concentrations of sucrose (10%, 20%, 30%) for 24 hours each or until the tissue sank to the bottom of the container. Brain tissue was sectioned coronally at 20 µm using a freezing microtome (Leica Microsystems Inc, IL). Sections were mounted onto microscope slides, and allowed to air dry. Slides were stained in 0.1% Cresyl violet solution for 5 minutes at 60˚C, rinsed in distilled water, dehydrated in 70% ethanol for 3 minutes, and coverslipped with Permount mounting medium (ThermoFischer Scientific, MA). Sections were examined using an Olympus CKX41 inverted microscope, and images were stitched with Microsoft Image Composite Editor.

SCG cells were labeled with tyrosine hydroxylase and neurofilament antibodies to confirm their sympathetic and neuronal identity, respectively. SCGs were removed, fixed in 4% paraformaldehyde in PBS for up to 24 hours at 4˚C, and cryoprotected in increasing concentrations of sucrose (10%, 20%, and 30%), for 24 hours each or until the tissue sank to the bottom. The SCG was sectioned at 10 µm using a freezing microtome and sections were mounted onto two separate microscope slides for immunodetection of neurofilament-containing cells and tyrosine hydroxylase-containing neurons. Slides were boiled in 0.1M citrate buffer pH 6, at 100˚C for 15 minutes, cooled for 15 minutes, and washed three times in PBS for 5 minutes each. Slides were incubated in blocking solution, 1X Tris-buffered saline with 0.05% Tween-20 (TBST), 20 mg/ml bovine serum albumin, and 5 mg/ml whole milk powder for 30 minutes at room temperature in a covered humid chamber. Immunodetection was performed using monoclonal primary antibodies diluted in blocking solution (anti-neurofilament antibody, 1:400, Sigma-Aldrich, St. Louis, MO; anti-tyrosine-hydroxylase antibody, 1:100, Sigma-Aldrich) overnight at 4˚C. After three washes in TBST for 5 minutes each, biotinylated secondary anti-mouse antibody was added (dilution 1:300, Vector Laboratories, Burlingame, CA) for 2 hours at room temperature. After 3 washes, secondary antibody staining was performed with fluorescein streptavidin or Texas Red streptavidin (dilution 1:200, Vector Laboratories) for 1 hour at room temperature. After three washes, sections were coverslipped with ProLong Gold anti-fade with DAPI (Invitrogen, NY). Sections were imaged on an Olympus FV-1000 confocal microscope and images were stitched together using Adobe Photoshop CS5.1.

Supplemental References

Akaike T (1982) Periodic bursting activities of locus coerulleus neurons in the rat. Brain Res 239:629-633.

Aston-Jones G, Chiang C, Alexinsky T (1991) Discharge of noradrenergic locus coeruleus neurons in behaving rats and monkeys suggests a role in vigilance. Prog Brain Res 88:501-520.

Bari BA, Ollerenshaw DR, Millard DC, Wang Q, Stanley GB (2013) Behavioral and Electrophysiological Effects of Cortical Microstimulation Parameters. PLoS ONE 8:e82170.

Devilbiss DM, Waterhouse BD (2004) The Effects of Tonic Locus Ceruleus Output on Sensory-Evoked Responses of Ventral Posterior Medial Thalamic and Barrel Field Cortical Neurons in the Awake Rat. The Journal of Neuroscience 24:10773-10785.

Nassar MR, Rumsey KM, Wilson RC, Parikh K, Heasly B, Gold JI (2012) Rational regulation of learning dynamics by pupil-linked arousal systems. Nat Neurosci 15:1040-1046.

Ollerenshaw Douglas R, Zheng He JV, Millard Daniel C, Wang Q, Stanley Garrett B (2014) The Adaptive Trade-Off between Detection and Discrimination in Cortical Representations and Behavior. Neuron 81:1152-1164.

Ollerenshaw DR, Bari BA, Millard DC, Orr LE, Wang Q, Stanley GB (2012) Detection of tactile inputs in the rat vibrissa pathway. J Neurophysiol 108:479-490.

Otsu N (1979) A Threshold Selection Method from Gray-Level Histograms. Systems, Man and Cybernetics, IEEE Transactions on 9:62-66.

Paxinos G, Watson C (2009) The rat brain in stereotaxic coordinates. Boston, MA: Elsevier Inc.

Vazey EM, Aston-Jones G (2014) Designer receptor manipulations reveal a role of the locus coeruleus noradrenergic system in isoflurane general anesthesia. Proceedings of the National Academy of Sciences 111:3859-3864.

Wang Q, Webber R, Stanley GB (2010) Thalamic Synchrony and the Adaptive Gating of Information Flow to Cortex. Nat Neurosci 13:1534-1541.

Wang Q, Millard DC, Zheng HJV, Stanley GB (2012) Voltage-sensitive dye imaging reveals improved topographic activation of cortex in response to manipulation of thalamic microstimulation parameters. Journal of Neural Engineering 9:026008.

Zheng HJV, Wang Q, Stanley GB (2015) Adaptive shaping of cortical response selectivity in the vibrissa pathway. Journal of Neurophysiology 113:3850-3865.